

Southward Migration of the Intertropical Convergence Zone Through the Holocene

Gerald H. Haug,¹ Konrad A. Hughen,² Daniel M. Sigman,³
Larry C. Peterson,⁴ Ursula Röhl⁵

is close to our determination for contaminant Pb at the North Pole (~1.179), lies within the range of Eastern European sources, and could signify the export of Pb from the Laptev Sea either in ice or water—a process that takes as little as 2 years (23). Finally, the Pb data suggest that the recent displacement of the front between the Atlantic and Pacific water masses into the Canadian Basin (Fig. 3) is unusual in that contaminant Pb, which may be transported there from the Laptev Sea under the present circulation regime (24), is simply not evident.

References and Notes

1. R. W. Macdonald et al., *Sci. Total Environ.* **254**, 93 (2000).
2. J. N. Smith, K. M. Ellis, L. R. Kilius, *Deep Sea Res. Part I* **45**, 959 (1998).
3. B. K. Schaule, C. C. Patterson, in *Trace Elements in Seawater*, C. S. Wong et al., Eds. (Plenum, New York, 1983), pp. 487–504.
4. E. A. Boyle, S. D. Chapnick, G. T. Shen, M. P. Bacon, *J. Geophys. Res.* **91**, 8573 (1986).
5. L. Y. Alleman, A. J. Véron, T. M. Church, A. R. Flegal, B. Hamelin, *Geophys. Res. Lett.* **26**, 1477 (1999).
6. A. Véron, C. E. Lambert, A. Isley, P. Linet, F. Grousset, *Nature* **326**, 278 (1987).
7. B. Hamelin, F. Grousset, E. R. Sholkovitz, *Geochim. Cosmochim. Acta* **54**, 37 (1990).
8. C. C. Patterson, D. M. Settle, *Mar. Chem.* **22**, 137 (1987).
9. B. Rudels, E. P. Jones, L. G. Anderson, G. Katner, in *The Polar Oceans and Their Role in Shaping the Global Environment*, vol. 85 of *Geophysical Monograph Series*, O. M. Johannessen, R. D. Muench, J. E. Overland, Eds. (American Geophysical Union, Washington, DC, 1994), pp. 33–46.
10. F. Schoster, M. Behrends, C. Müller, R. Stein, M. Wahsner, *Int. J. Earth Sci.* **89**, 486 (2000).
11. D. A. Darby, J. F. Bishop, G. A. Jones, *Deep Sea Res. Part II* **44**, 1745 (1997).
12. M. Murozumi, T. J. Chow, C. C. Patterson, *Geochim. Cosmochim. Acta* **33**, 1247 (1969).
13. S. Hong, J.-P. Candelone, C. C. Patterson, C. F. Boutron, *Science* **265**, 1841 (1994).
14. F. A. Akeredolu et al., *Atmos. Environ.* **28**, 1557 (1994).
15. A. J. Véron, T. M. Church, *J. Geophys. Res.* **102**, 28049 (1997).
16. F. Monna, J. Lancelot, I. W. Croudace, A. B. Cundy, J. T. Lewis, *Environ. Sci. Technol.* **31**, 2277 (1997).
17. J. F. Hopper, H. B. Ross, W. T. Sturges, L. A. Barrie, *Tellus* **43B**, 45 (1991).
18. W. T. Sturges, J. F. Hopper, L. A. Barrie, R. C. Schnell, *Atmos. Environ.* **27A**, 2865 (1993).
19. H. D. Livingston, *Philos. Trans. R. Soc.* **25**, 161 (1988).
20. U. Schauer et al., *Ann. Geophys.*, in press.
21. H. Eicken et al., *Geophys. Res. Lett.*, **27**, 1919 (2000).
22. A. J. Véron, T. M. Church, I. Rivera-Duarte, A. R. Flegal, *Deep Sea Res. Part II* **46**, 919 (1999).
23. I. Rigor, *ARCOS Newsl.* **44**, 1 (1992).
24. A. Y. Proshutinsky, M. A. Johnson, *J. Geophys. Res.* **102**, 12493 (1997).
25. A. Ng, C. C. Patterson, *Geochim. Cosmochim. Acta* **46**, 2307 (1982).
26. Y. Erel, Y. Dubowski, L. Halicz, J. Erez, A. Kaufman, *Environ. Sci. Technol.* **35**, 292 (2001).
27. J. N. Smith, K. M. Ellis, T. M. Boyd, *J. Geophys. Res.* **104**, 29663 (1999).
28. W. M. Smethie Jr., P. Schlosser, T. S. Hopkins, G. Boenisch, *J. Geophys. Res.* **105**, 1105 (2000).
29. J. Morison, M. Steele, R. Andersen, *Deep Sea Res. Part I* **45**, 15 (1998).
30. Copyright, Her Majesty in right of Canada, as represented by the Minister of Fisheries and Oceans.
31. We thank R. Shearer and D. Stone for the Canadian Northern Contaminants Program; the U.S. Office of Naval Research for funding support (J.N.S.); and D. Paton for technical assistance at sea.

2 May 2001; accepted 2 July 2001

Titanium and iron concentration data from the anoxic Cariaco Basin, off the Venezuelan coast, can be used to infer variations in the hydrological cycle over northern South America during the past 14,000 years with subdecadal resolution. Following a dry Younger Dryas, a period of increased precipitation and riverine discharge occurred during the Holocene “thermal maximum.” Since ~5400 years ago, a trend toward drier conditions is evident from the data, with high-amplitude fluctuations and precipitation minima during the time interval 3800 to 2800 years ago and during the “Little Ice Age.” These regional changes in precipitation are best explained by shifts in the mean latitude of the Atlantic Intertropical Convergence Zone (ITCZ), potentially driven by Pacific-based climate variability. The Cariaco Basin record exhibits strong correlations with climate records from distant regions, including the high-latitude Northern Hemisphere, providing evidence for global teleconnections among regional climates.

The Cariaco Basin, an anoxic marine basin on the northern shelf of Venezuela, is a highly sensitive recorder of past climates in the tropical ocean (1–4), in part because its position causes it to accumulate sediments of both marine and terrestrial origin. At ~10°N, the basin sits at the northern edge of the annual latitudinal range of the ITCZ, with the ITCZ nearly overhead during the summer. During this season, rain falls in regions that drain directly into the Cariaco Basin or that contribute to flow in the Orinoco River (5). The subsequent runoff transports terrigenous materials to the coast and offshore, where they accumulate in sediments of the Cariaco Basin and surrounding shelf (3). During the winter/spring, when the ITCZ is located over the equator or further south, local river runoff is diminished, and the northeast trade winds shift south and intensify over the Cariaco Basin (5). These strong winds drive upwelling along the Venezuelan coast that feeds biological production in Cariaco surface waters, delivering organic matter and calcareous and siliceous microfossils to the seafloor. This seasonal alternation between river runoff and upwelling is recorded in the lamination of the Cariaco sediments, with dark-colored terrigenous grain-rich layers deposited during the rainy summer/fall and lighter-

colored biogenic-rich layers deposited during the windy winter/spring (Fig. 1). The absence of oxygen in deep basin waters prevents bioturbation, resulting in a continuous, largely laminated sediment sequence spanning the last 14.5 thousand years (ky) (1, 2).

Ocean Drilling Program (ODP) Site 1002 (10°42.73'N, 65°10.18'W) was drilled at a water depth of 893 m (6), well below the depth (~300 m) at which oxygen-free conditions in the Cariaco water column currently begin. We report on the uppermost 5.5 m of the 170-m sediment sequence recovered at Hole 1002C, which covers the last 14 ky. The laminated nature of the sediments and the high deposition rates (~30 cm/ky) in this natural sediment trap yield an important tropical counterpart to high-latitude ice cores for the study of climate change at interannual to millennial time scales. Detailed age control is based on a series of 10 accelerator mass spectrometry (AMS) ¹⁴C dates of the planktic foraminifer *Globigerina bulloides*, all transferred to calendar years using the calibration of (7).

Bulk sedimentary iron (Fe) and titanium (Ti) were measured over this interval at 2 mm spacing, corresponding to a sampling interval of ~4 to 5 years, with a profiling x-ray fluorescence scanner at the University of Bremen (Figs. 2 and 3) (8). This represents the maximum resolution of this new instrument. In our 14-ky-long record, Ti and Fe concentrations were generally low in sediments deposited during the Younger Dryas cold period between 12.6 and 11.5 thousand years ago (ka). Their concentrations increased during the “Pre-boreal” period (11.5 to 10.5 ka) and were

¹Department of Earth Sciences, Eidgenössische Technische Hochschule—Zentrum, CH-8092 Zürich, Switzerland. ²Woods Hole Oceanographic Institution, Woods Hole, MA 02543, USA. ³Department of Geosciences, Princeton University, Princeton, NJ 08544, USA. ⁴Rosenstiel School of Marine and Atmospheric Science, University of Miami, Miami, FL 33149, USA. ⁵Fachbereich Geowissenschaften, Universität Bremen, D-28334 Bremen, Germany.

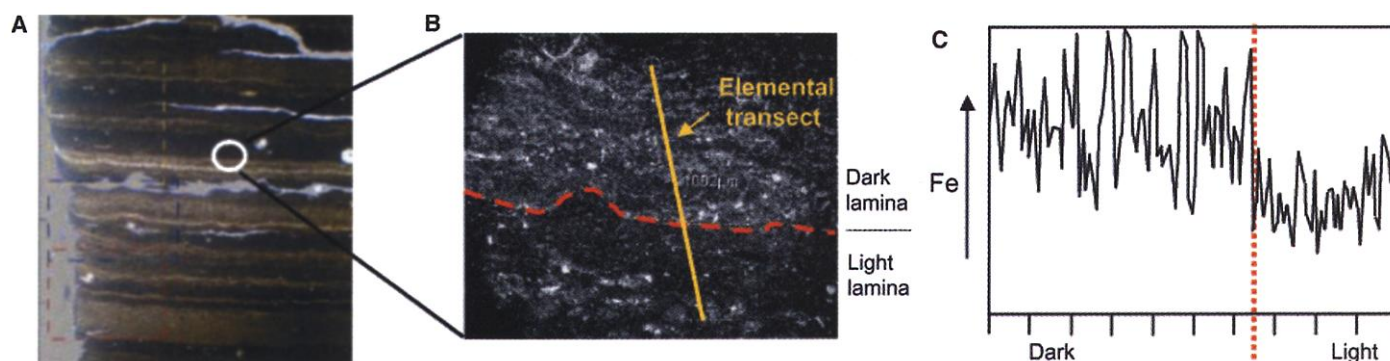


Fig. 1. Relation between sediment laminae and Fe content in Cariaco Basin sediments, based on an x-ray transect from a sediment thin section. (A) Optical micrograph of well-developed laminae in Cariaco Basin from core PL07-56 PC (476 to 479 cm). Dark-colored laminae are rich in silt and clay deposited during the local rainy season. Light-colored laminae are rich in biogenic silica and carbonate deposited during the drier (winter/spring) upwelling season. (B) Backscattered electron image

(SEM) of the laminae contact indicated in (A). Note that light laminae appear dark and dark laminae appear light in this image. (C) Results of x-ray analysis of the Fe content of these sediments along the transect location indicated in Fig. 1B. Fe is clearly concentrated in the dark-colored laminae and dominantly reflects riverine input of terrigenous sediment to the Cariaco Basin during the summer/fall rainy season. [Data courtesy of M. Scherer]

highest during the Holocene “thermal maximum” (10.5 to 5.4 ka), with a subsequent long-term decrease. Superimposed on these trends are shorter term variations ranging from millennia to decades in length. High Ti and Fe values during the Holocene “thermal maximum” were interrupted by lower values between 8.3 and 7.8 ka, followed by another minimum centered at ~5 ka. In sediments deposited between ~3.8 and 2.8 ka, the overall amplitude of the fluctuations increases markedly, with four pronounced minima in Fe and Ti concentrations centered at ~3.8, 3.4, 3.0, and 2.8 ka. Finally, a minimum characterizes the period between 550 and 200 years ago, corresponding to the timing of the recent “Little Ice Age.”

Although the Fe variations alone could perhaps be attributed to redox changes in the sediment, Ti is insensitive to environmental redox variations (9) and shows a downcore pattern very similar to Fe (Fig. 2). In addition, the presence of laminae and the near-total absence of a benthic microfauna indicate that the basin has been continuously anoxic throughout the last 14 ky. Hence, Fe and Ti variations in the Cariaco Basin are not diagenetically controlled, and either element can be interpreted to reflect changes in terrigenous sediment input (3).

As a simple chemical proxy for the input of land-derived materials, Fe and Ti variations provide a direct measure of rainfall and runoff from local watersheds (3, 5). At the scale of individual laminae, this assertion is supported by compositional analysis of the sediment couplets that record the seasonally varying input to the basin (Fig. 1). Independent paleoclimatic data also support our use of Fe and Ti variations as indices of regional hydrologic change. For example, the Younger Dryas cold period, marked by low metal concentrations in the Cariaco Basin (Figs. 2 and 3), was a time of reduced precipitation

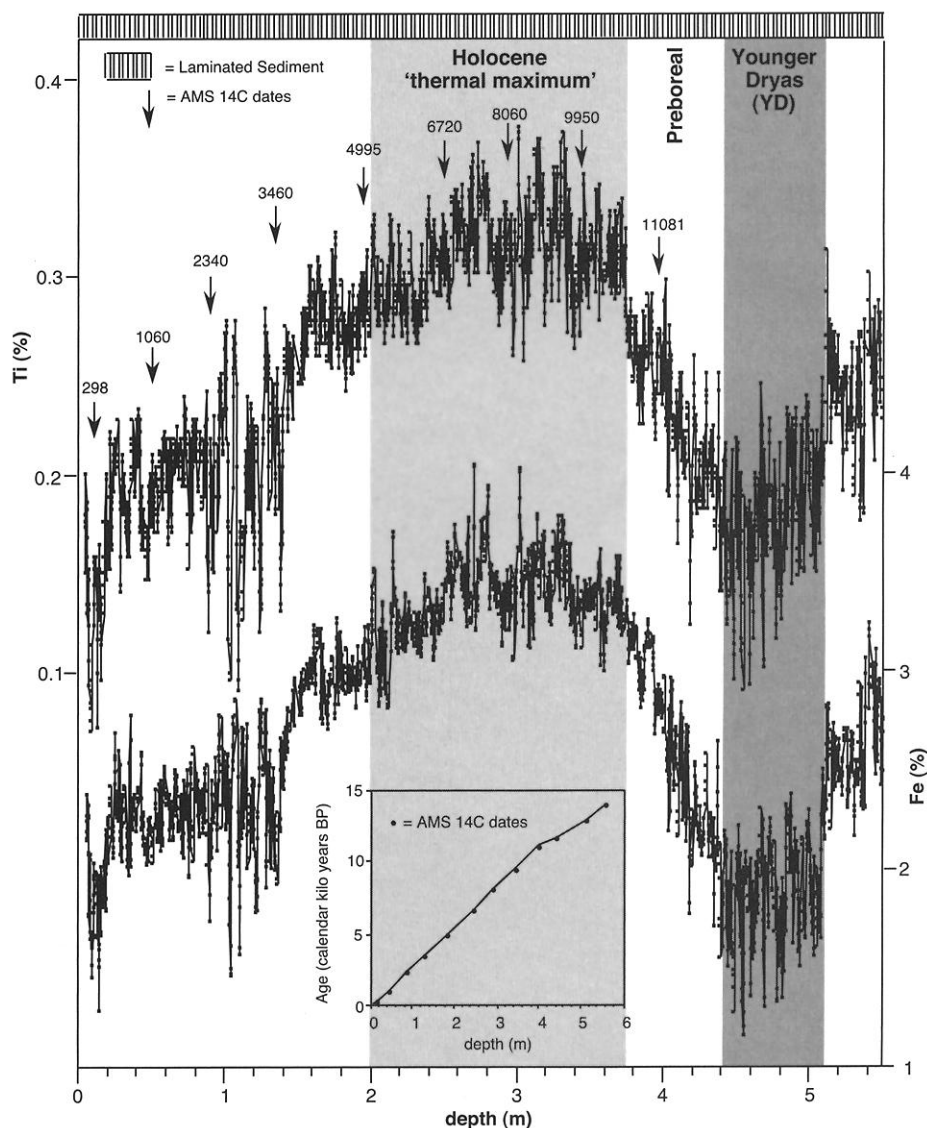


Fig. 2. Cariaco Basin metal concentrations (Fe, Ti) versus core depth (m) in ODP Site 1002 (data smoothed by a 3-point running mean). Arrows indicate the position of AMS ^{14}C dates converted to calendar years before the present (BP). Inset: Depth-age plot showing sedimentation rates over the time period of this study.

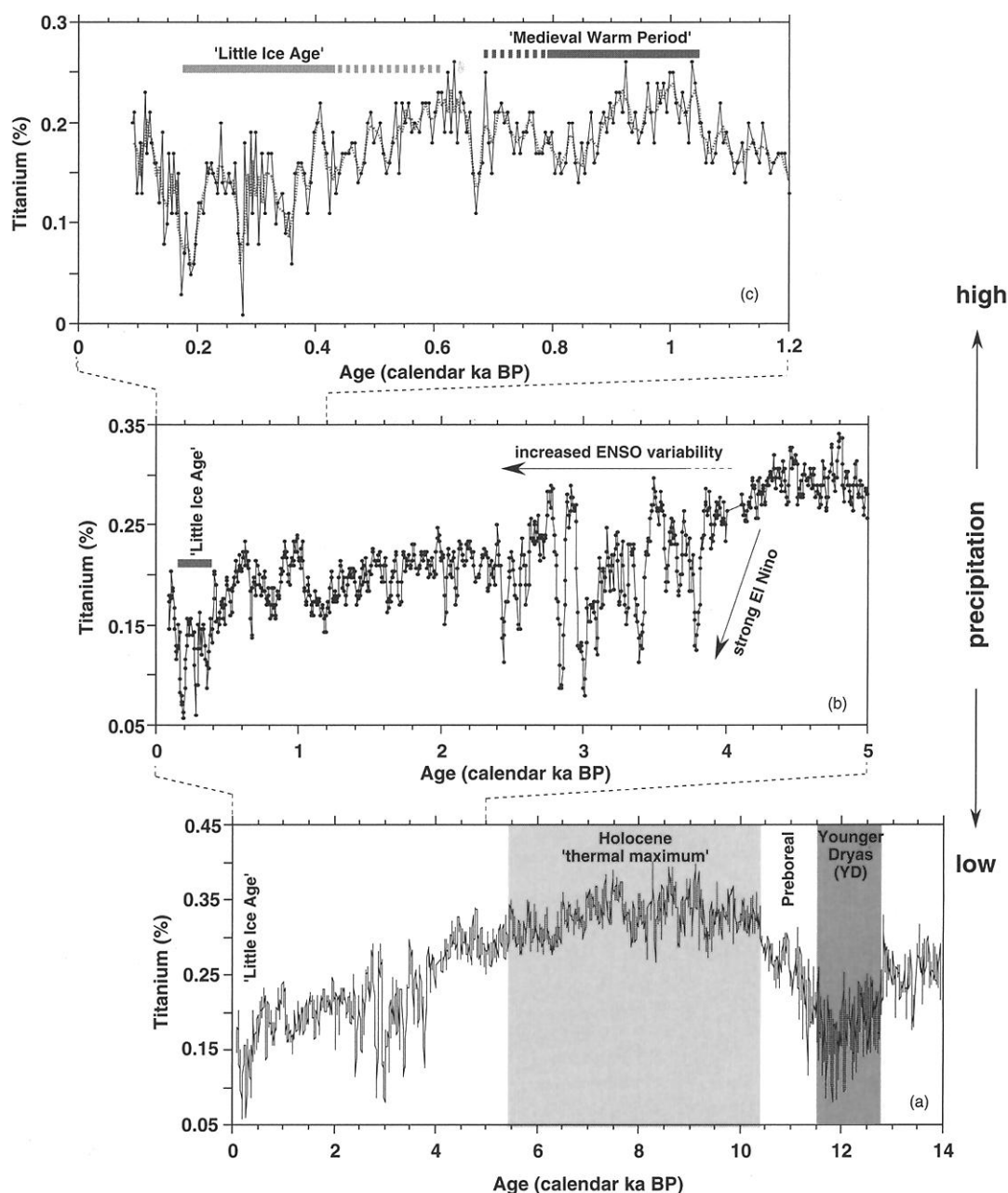
over much of the tropical Atlantic, as indicated by lake-level data from west Africa (10), pollen data from northern South America (11), and general circulation model (GCM) simulations of regional climate during this period (12). The wettest conditions of the last 14 ky, as inferred from high Fe and Ti values, occurred between 10.5 and 5.4 ka during the Holocene "thermal maximum," a period associated with wet conditions in Africa (10, 13) and with the most depleted oxygen isotope values in Cariaco Basin foraminifera (14). The subsequent Holocene drying trend has been previously recognized in a lacustrine record from Haiti (15) and in pollen records from nearby Lake Valencia (16), affirming the broad regional importance of the Cariaco Basin sediment record. Sea level,

which plays a major role in modulating terrigenous input to this basin on glacial-interglacial time scales (6), has probably not varied so much during the Holocene as to influence Fe and Ti concentrations over the interval of this study (17).

Large century-scale variations in precipitation are inferred between ~3.8 and 2.8 ka, based on amplitudes of the Fe and Ti signals that are comparable to the difference between the Younger Dryas and the Holocene "thermal maximum." Higher but variable precipitation is also indicated from 1.05 to 0.7 ka, the interval of time sometimes referred to as the "Medieval Warm Period." This was followed by the "Little Ice Age," marked by drier conditions in the Cariaco region and punctuated by three notable precipitation minima.

Although independent evidence supports our interpretation of the metal data in terms of precipitation and runoff, Fe and Ti contents can also vary as a result of dilution by biogenic sediment components. Calcium carbonate, derived mostly from coccolithophorids and planktic foraminifera, typically makes up 25 to 35% of the Holocene sediments at Site 1002 (6). Diatoms are locally important as well (18). Tradewind-driven upwelling is the dominant cause for changes in Cariaco biological export production during the Holocene (1). Hence, changes in upwelling might be expected to affect the sedimentary concentrations of Ti and Fe through dilution, leading to ambiguity in the interpretation of the metal data in the absence of additional information. However, bulk accu-

Fig. 3. Bulk Ti content of Cariaco Basin sediments from ODP Site 1002 versus age, spanning (a) the last 14 ky (3-point running mean); (b) the last 5 ky (3-point running mean); and (c) the last 1.2 ky (raw data and 3-point running mean). Higher Ti content reflects greater terrigenous input from riverine runoff and is interpreted to indicate greater precipitation and a more northerly mean latitude of the ITCZ.



mulation rates have held remarkably constant over the past 11 ky (Fig. 2) despite the roughly 50% decrease in Ti content over the past 8 ky. Given that biogenic and terrigenous components account for roughly equal fractions of the sediment, the constancy of total sediment accumulation in the face of known compositional changes requires that the deposition of biogenic and terrigenous sediments be counterbalanced, with increases in one associated with decreases in the other.

What single environmental parameter can explain this relation between seemingly unrelated sedimentary fractions? We argue that the mean latitudinal position of the ITCZ is this variable, dynamically linking changes in the accumulation of biogenic and terrigenous sediment through its coupled effects on precipitation and wind-driven upwelling. As already noted, a clear record of the seasonal migration of the ITCZ is preserved in the elemental composition of the sediment varves in the Cariaco Basin. Given the constant overall sedimentation rates of the last 11 ky, it is most probable that longer term changes in sediment composition observed at Site 1002 are similarly controlled by the latitude of the ITCZ. In this view, the high Ti and Fe concentrations associated with the Holocene "thermal maximum" would indicate a more northerly mean annual position for the ITCZ relative to the later Holocene, causing both more precipitation and less tradewind-driven upwelling in the Cariaco region.

Strong support for ITCZ migration as the dominant driver of Holocene variations in the Cariaco metal records comes from comparison with climate records that provide a Southern Hemisphere complement to our Northern Hemisphere record. To the south, new sediment records from Lake Titicaca indicate that precipitation steadily increased in that region between 4 and 2.4 ka and again during the "Little Ice Age" (19). Pollen records from the southern margin of Amazonia also suggest a southward expansion of humid evergreen forest during the late Holocene (20). These changes are anticorrelated with decreases in precipitation indicated in the Cariaco record, together confirming that these climate events were associated with southward movements of the ITCZ.

A general southward shift of the ITCZ over the course of the Holocene may have resulted from changes in the seasonality of insolation associated with the ~21-ky precession component of Milankovitch forcing. During the late Holocene, Southern Hemisphere insolation has become more seasonal while Northern Hemisphere insolation has become less seasonal (21). This should have decreased the capacity of the northern summer insolation maximum to pull the ITCZ off the equator while increasing it to the south, reducing summertime rainfall near the Cariaco Basin while increasing it over the Ama-

zon (20, 22), exactly as observed.

Despite evidence for a southward shift over time, the continued bias of the ITCZ to the Northern Hemisphere near the Americas today results from the preferential cooling of surface waters in the southern east equatorial Pacific by upwelling, which displaces the sea surface temperature maximum (and thus the zone of convergence) into the Northern Hemisphere (21). During warm El Niño events, the exposure of cold subsurface waters in the eastern equatorial Pacific is greatly reduced, and the temperature structure of the region becomes more symmetric about the equator. As a result, El Niño events are characterized by a mean southward shift of the ITCZ in the Pacific basin (23), as well as by dry conditions in northern South America (5, 24). Indeed, the insolation changes noted above, while directly forcing a southward migration of the ITCZ, may also have increased the prevalence of El Niño through the Holocene (25), further amplifying the southward shift in the ITCZ while adding a higher frequency component to its latitudinal variations.

Supporting evidence for an increase in El Niño-like conditions in the late Holocene comes from both paleoclimatic reconstructions and modeling studies (25). Geoarchaeological evidence from northern Peru suggests a major climate change at ~5 ka, with an increase in El Niño–Southern Oscillation (ENSO) activity thereafter (26). Storm deposits in an alpine lake in Ecuador similarly suggest that modern ENSO periodicities were established after ~5 ka, with the highest spectral density at El Niño frequencies occurring between ~3.5 and 2.6 ka and during the last 660 years (27). Independent evidence from northern Australia also suggests that ENSO became active only after ~5 ka (28). Although the age control and temporal resolution of these records could be improved, and the evidence in some cases is indirect, existing data from widely scattered sites nevertheless point to a marked increase in ENSO activity in the late Holocene whose onset approximates the major change in character of the Cariaco Basin metal records after ~3.8 ka. We cannot be certain that the higher frequency variability in the Cariaco record after 3.8 ka is a result of ITCZ migration, but a good correlation between the Site 1002 data and new tree ring records from Tasmania (29) suggests a dynamical link between variability in the two regions, best explained by the coupled response of climate parameters that are sensitive to ENSO, such as the latitudinal position of the ITCZ.

The position of the ITCZ over northern South America is also influenced by Atlantic sea surface conditions, making changes in the temperature gradient of the Atlantic an alternative driver for some component of the ITCZ variation (2, 4, 12, 30). This may explain the coincidence between cold peri-

ods in the high-latitude North Atlantic (31) and drier conditions over northern South America, particularly during the Little Ice Age. Even the internal structure of the broad Ti minimum of the Little Ice Age (Figs. 2 and 3), with its three distinct sub-minima, is reminiscent of periods of increased North Atlantic storminess recorded by sea salt in the Greenland Ice Sheet Project GISP II ice core (32). However, determining causation from these coincidences is not yet possible. It may well be that the ITCZ migration and Northern Hemisphere cooling are both consequences of climate forcing in the Pacific or some other region.

The Cariaco record, when combined with other records from South America (19, 20, 22), unambiguously shows that climate changes in Central and South America over the course of the Holocene are due at least in part to a general southward shift of the ITCZ (34). This migration can be explained by the Holocene history of insolation, both directly and through its effect on tropical Pacific sea surface conditions (23). The correlation of the Cariaco Basin sediment record with historical records (33) and with paleorecords of climate change in regions bordering the Atlantic and Pacific (26–29, 31–33) is evidence for large-scale linkages that propagate regional climate changes around the globe. The Pacific, given its areal extent and the energetic importance of its equatorial upwelling (35), deserves major consideration as the conductor of these global climate oscillations.

References and Notes

1. L. C. Peterson, J. T. Overpeck, N. G. Kipp, J. Imbrie, *Paleoceanography* **6**, 99 (1991).
2. K. A. Hughen, J. T. Overpeck, L. C. Peterson, S. E. Trumbore, *Nature* **380**, 51 (1996).
3. L. C. Peterson, G. H. Haug, K. A. Hughen, U. Röhl, *Science* **290**, 1947 (2000).
4. D. E. Black et al., *Science* **286**, 1709 (1999).
5. S. Hastenrath, L. Greishar, *J. Geophys. Res.* **98**, 5093 (1993).
6. L. C. Peterson et al., *Proc. ODP Sci. Res.* **165**, 85 (2000).
7. M. Stuiver et al., *Radiocarbon* **40**, 1041 (1998).
8. U. Röhl, L. J. Abrams, *Proc. ODP Sci. Res.* **165**, 191 (2000).
9. K. M. Yarinick, R. W. Murray, L. C. Peterson, *Paleoceanography* **15**, 210 (2000).
10. COHMAP Members, *Science* **241**, 1043 (1988).
11. T. van der Hammen, H. Hooghiemstra, *Quat. Sci. Rev.* **14**, 841 (1995).
12. D. Rind et al., *Clim. Dyn.* **1**, 33 (1986).
13. P. deMenocal, J. Ortiz, T. Guilderson, M. Sarnthein, *Science* **288**, 2198 (2000).
14. H.-L. Lin et al., *Paleoceanography* **12**, 415 (1997).
15. D. A. Hodell et al., *Nature* **352**, 790 (1991).
16. J. P. Bradbury et al., *Science* **214**, 1299 (1981).
17. R. G. Fairbanks, *Nature* **342**, 637 (1989).
18. R. C. Thunell et al., *Limnol. Oceanogr.* **45**, 300 (2000).
19. P. A. Baker et al., *Science* **291**, 640 (2001).
20. F. E. Mayle, R. Burbridge, T. J. Killeen, *Science* **290**, 2291 (2000).
21. A. Berger, M. F. Loutre, *Quat. Sci. Rev.* **10**, 297 (1991).
22. M. A. Maslin, S. J. Burns, *Science* **290**, 2285 (2000).
23. A. V. Fedorov, S. G. Philander, *Science* **288**, 1997 (2000).
24. K. E. Trenberth et al., *J. Geophys. Res.* **103**, 14291 (1998).
25. A. C. Clement, R. Seager, M. A. Cane, *Paleoceanography* **15**, 731 (2000).

26. D. H. Sandweiss et al., *Science* **273**, 1531 (1996).
27. D. T. Rodbell et al., *Science* **283**, 516 (1999).
28. M. S. McGlone, A. P. Kershaw, V. Markgraf, in *El Niño: Historical and Paleoclimatic Aspects of the Southern Oscillation*, H. F. Diaz, V. Markgraf, Eds. (Cambridge Univ. Press, Cambridge, 1992), pp. 435–462.
29. E. R. Cook, B. M. Buckley, R. D. D'Arrigo, M. J. Peterson, *Clim. Dyn.* **16**, 79 (2000).
30. P. Chang, L. Ji, H. Li, *Nature* **385**, 516 (1997).
31. K. R. Briffa et al., *Clim. Dyn.* **7**, 111 (1992).
32. S. R. O'Brien et al., *Science* **270**, 1962 (1995).
33. D. A. Hodell, M. Brenner, J. H. Curtis, T. Guilderson, *Science* **292**, 1367 (2001).
34. See supplemental figure at Science Online (www.sciencemag.org/cgi/content/full/293/5533/1304/DC1).
35. M. Cane, A. C. Clement, *Geophys. Monogr.* **112**, 373 (1999).
36. We thank D. Ariztegui, M. Cane, C. Charles, A. Clement, H. Cullen, W. Curry, D. Hodell, T. Joyce, L.

Keigwin, T. Stocker, H. Thierstein, D. Oppo, G. Philander, and two anonymous reviewers for discussions and helpful comments. We also thank M. Scherer for scanning electron microscopy (SEM) and x-ray results shown in Fig. 1 that arose from a class project at the University of Miami. Supported by the Deutsche Forschungsgemeinschaft and NSF.

9 February 2001; accepted 12 July 2001

Queen Control of Sex Ratio in Fire Ants

L. Passera,¹ S. Aron,² E. L. Vargo,³ L. Keller^{4*}

The haplodiploid sex-determination system of ants gives rise to conflict between queens and workers over colony sex ratios, and the female-biased allocation ratios seen in many species suggest that workers often prevail in this conflict. We exchanged queens between male- and female-specialist colonies of the fire ant *Solenopsis invicta*. These exchanges quickly reversed the sex-ratio biases of adopting colonies. The sex ratio of queen-laid eggs differed strongly between male- and female-specialist colonies. These findings suggest that queens can force workers to raise male sexuals by limiting the number of female brood and help to explain why sex investment ratios lie between the queen and worker equilibria in this and many other ant species.

Social insects provide some of the most striking examples of elaborate cooperative behavior, yet life within colonies also entails conflicts (1–5). In ants, the most strident conflict concerns sex ratio, with workers favoring a more female-biased sex investment ratio than queens (1). This conflict arises because of the hymenopteran haplodiploid system of sex determination, whereby unfertilized eggs develop into males and fertilized eggs into females (1). As a result, workers in colonies headed by a single once-mated queen are three times more related to sisters ($r = 0.75$) than to brothers ($r = 0.25$). Because of this asymmetry in relatedness, the population-wide sex allocation ratio should equilibrate at 3:1 (female:male) if workers control the colony's investment in reproductive offspring. By contrast, because queens are equally related to their daughters and sons, an equal investment in male and female reproductives is expected if the colony's allocation of resources is under the control of the queen.

Sex ratios have been studied in many ants, and, across species, population-wide sex allocation ratios lie between the queens' and

workers' equilibria (1–3, 6–8). Because they control brood rearing and food flow in the colony, workers can bias sex allocation, for example, by selectively eliminating males and/or preferentially feeding females. Workers have indeed been shown to manipulate colony sex ratios by selectively eliminating male brood in some ants (9–13). Studies of species in which variation in social organization leads to intercolonial differences in relatedness asymmetries also reveal that workers in some species bias sex ratios adaptively by favoring sex allocation in females in those colonies with relatedness asymmetries greater than the population average (e.g., those headed by one singly mated queen) and favoring the production of males in colonies with lower than average relatedness asymmetries (e.g., those with multiply mated queens or several related queens) (14, 15). The fact that population-wide sex allocation is less female-biased than the workers' equilibrium or close to the queen equilibrium in some species (16) suggests that workers do not exert complete control over sex allocation but that queens have some measure of control over sex-ratio allocation in some social Hymenoptera. The mechanisms by which queens may exert this control have remained elusive (2, 16–18).

Here we test the hypothesis that queens may bias sex ratios toward males by limiting the number of female eggs in the colony (16–21), using the fire ant *Solenopsis invicta*, one of the best studied social insects (22). Colonies of the monogyne form of this spe-

cies consist of one singly mated queen and her daughter workers that are completely sterile (23). This simple family structure leads to uniformly high relatedness asymmetry (3:1) and workers favoring an investment in females three times higher than queens. In this species, colonies produce mostly individuals of a single sex (24–26). To test whether sex-ratio specialization is induced by queens or workers, we made use of the fact that colonies made queenless will usually accept a new unfamiliar queen (27). The ability to conduct cross-fostering experiments, where queens are transferred between male- and female-specialist colonies, provides an opportunity to determine the extent to which queens or workers control colony sex ratios in a social insect.

We selected 24 field colonies with highly biased sex ratios in a monogyne population (28). Eleven of these colonies were male specialists (numerical proportion of males, range: 0.77 to 1.0), and 13 were female specialists (numerical proportion of males, range: 0.0 to 0.09). The queen in each colony was exchanged with the queen from another colony, producing sexuals of the other sex (experimental colonies) or sexuals of the same sex (control colonies). Twenty-two of the 24 colonies accepted the foreign queen, and 21 of these colonies produced a new batch of reproductives 5 weeks after queen exchange. Male-specialist colonies that were given a queen from a female-specialist colony switched to producing mostly or only females (Fig. 1; $t_5 = 16.14$, $P < 0.0001$, paired t test). Conversely, female-specialist colonies that received a queen from a male-specialist colony switched to producing males (Fig. 1; $t_4 = 8.94$, $P < 0.001$, paired t test). By contrast, no significant change in sex ratio occurred in control colonies in which male-specialist and female-specialist colonies were given a queen from the same colony type (male specialist, $t_3 = 0.67$, $P = 0.55$, paired t test; female specialist, $t_5 = 0.54$, $P = 0.61$, paired t test). The fact that colony sex ratios are predominantly influenced by queens is also demonstrated by the significant correlation between the sex ratio produced by a queen's original colony and the sex ratio produced by the recipient colony 5 to 6 weeks after the queen was introduced (experimental colonies: $r^2 = 0.77$, $n = 10$, $P < 0.001$; control colonies: $r^2 = 0.92$, $n =$

¹Laboratory of Ethology and Animal Cognition, FRE-CNRS 2382, University Paul-Sabatier, Toulouse Cedex 31062, France. ²Unit of Animal Communities, Free University of Brussels, Brussels 1050, Belgium. ³Department of Entomology, Campus Box 7613, North Carolina State University, Raleigh, NC 27695–7613, USA. ⁴Institute of Ecology, University of Lausanne, Lausanne 1015, Switzerland.

*To whom correspondence should be addressed. E-mail: Laurent.keller@ie-zea.unil.ch